Article

Not peer-reviewed version

SILAC-Based Characterization of Plasma-Derived Extracellular Vesicles in Patients Undergoing Partial Hepatectomy

Ulrike Resch *, Hubert Hackl, David Pereyra, Jonas Santol, Laura Brunnthaler, Joel Probst, Anna Sofie Jankoschek, Monika Aiad, Hendrik Nolte, Marcus Krueger, Patrick Starlinger, Alice Assinger *

Posted Date: 30 August 2024

doi: 10.20944/preprints202408.2181.v1

Keywords: Liver regeneration; extracellular vesicles; biomarkers; proteomics; post hepatectomy liver failure

Article

SILAC-Based Characterization of Plasma-Derived Extracellular Vesicles in Patients Undergoing Partial Hepatectomy

Ulrike Resch [1,2,*], Hubert Hackl [3], David Pereyra [4], Jonas Santol [4], Laura Brunnthaler [1], Joel Probst [4], Anna Sofie Jankoschek [4], Monika Aiad [4], Hendrik Nolte [2], Marcus Krueger [2], Patrick Starlinger [3,4,5] and Alice Assinger [1,*]

1 Department of Vascular Biology and Thrombosis Research, Centre of Physiology and Pharmacology, Medical University of Vienna, Schwarzspanierstrasse 17, 1090 Vienna, Austria
2 CECAD, Proteomics Core Facilities, University of Cologne, Joseph-Stelzmann Strasse 26, D-50931 Cologne, Germany; uresch1@uni-koeln.de
3 Institute of Bioinformatics, Biocenter, Medical University of Innsbruck, Innsbruck, Austria
4 Department of Surgery, General Hospital, Medical University of Vienna, Währinger Gürtel 18-20, A-1090 Vienna, Austria
5 Department of Surgery, Division of Hepatobiliary and Pancreatic Surgery, Mayo Clinic, Rochester, MN, USA
* Correspondence: ulrike.resch@meduniwien.ac.at, Tel.: ++43-1-40160-31171 (U.R.); alice.assinger@meduniwien.ac.at, Tel.; ++43-1-40160-31420 (A.A.)

Abstract: Post-hepatectomy liver failure (PHLF) remains a significant risk for patients undergoing partial hepatectomy (PHx). Reliable prognostic markers and treatments to enhance liver regeneration are lacking. Plasma nanoparticles, including lipoproteins, exosomes, and extracellular vesicles (EVs), can reflect systemic and tissue-wide proteostasis and stress, potentially aiding liver regeneration. However, their role in PHLF is still unknow. *Methods:* Our study included 9 patients with hepatocellular carcinoma (HCC) undergoing PHx: 3 patients with PHLF, 3 patients undergoing the Associating Liver Partition and Portal vein Ligation for Staged hepatectomy (ALPPS) procedure and three matched controls without complications after PHx. Patient plasma was collected before (PRE), 1 and 5 days (POD1, POD5) after PHx. EVs were isolated by ultracentrifugation and extracted proteins subjected to quantitative mass spectrometry using a super-SILAC mix prepared from primary and cancer cell-lines. *Results:* We identified 2625 and quantified 2570 proteins in EVs in PHx patients. Among these, 53 proteins were significantly upregulated and 32 were downregulated in patients with PHLF compared to those without PHLF. Furthermore, 110 proteins were upregulated and 78 were downregulated in PHLF compared to patients undergoing ALPPS. The EV-proteomic signature in PHLF indicates significant disruptions in protein translation, proteostasis, intracellular vesicle biogenesis, as well as alterations in proteins involved in extracellular matrix (ECM) remodeling, metabolic and cell cycle pathways, present already before PHx. *Conclusion:* Longitudinal proteomic analysis of EV´s circulating in human patient plasma undergoing PHx uncovers proteomic signatures associated with PHLF which reflect dying hepatocytes and endothelial cells and are present before PHx already. Our results support EVs as potential biomarkers and therapeutic targets for liver regeneration and failure.

Keywords: liver regeneration; extracellular vesicles; biomarkers; proteomics; post hepatectomy liver failure

1. Introduction

The liver is the largest solid organ in the body fulfilling essential functions in synthesis, metabolism and distribution of protein, lipid, metabolites and hormones via secretion into the blood. The liver´s unprecedented capacity to regenerate, already described in the Ancient Greek mythology, acts as a rheostat to compensate for tissue injury caused by unfavorable life style or environmental

 doi:10.20944/preprints202408.2181.v1

exposure to toxic compounds for example. However, chronic tissue damage gives rise to liver cancer, which is the sixth most common cancer worldwide. For these patients, partial hepatectomy (PHx) is the primary therapeutic approach, but insufficient hepatic regeneration can lead to post hepatectomy liver failure (PHLF), which remains a significant clinical concern associated with patient morbidity and mortality [1]. Despite recent advances in prediction tools [2–5] prognostic markers to reliably predicting clinical outcome following surgery are lacking. During the past decade, research on the molecular mechanisms of liver regeneration gradually uncovered a highly complex and tightly regulated sequence of events necessary for tissue repair [6] and a range of regenerative growth factors and mediators have been identified. These are released from the liver tissue itself or from myeloid cells in response to surgical intervention. An unknown proportion of secreted molecules are packed into micro-nanosized (40nm up to 1um) lipid membrane *encircled* particles, termed extracellular vesicles (EVs). An increasing number of bioanalytical studies show that EVs are charged with proteins, nucleic acids and metabolites reflecting the donor cell-phenotype at the particular condition of their release [7,8]. Being released into the extracellular space and further into blood circulation, EVs fulfill important immunological and tissue homeostatic functions by mediating communication between cells (immune, parenchymal, stromal) and tissue, distant from their origin [9]. Their cargo is increasingly recognized to infer disease-specific processes, including cardiovascular, metabolic, neuropathogenic and oncogenic signatures [10–14] as well as ageing [15]. Building on these studies, the therapeutic application of EVs is actively being explored [16], including as treatment option for liver failure [17]. To date, 57 studies have demonstrated that EVs and their cargoes serve as reliably biomarkers and effective treatment options, at least in animal model and in *in vitro* systems.

Despite of the growing interest in EV research, an unbiased longitudinal proteomic analysis of EV´s circulating in human patient plasma following PHx has not been described so far. Anticipating inter and intra-patient heterogeneity, we utilized a custom made super-SILAC-mix to compare EVs from patients stratified on the basis of i) post-surgical outcome and ii) sampling time with the aim to identify etiologic factors promoting liver regeneration.

2. Results

2.1. Study Overview and Patient Characteristics

We included 9 patients with hepatocellular carcinoma (HCC) admitted to PHx which were analysed in regard to PHx outcome (PHLF or noPHLF, ALPPS) and in addition in regard to sampling time (PRE-POD1 and POD5). All patients (7 male, 2 female, average age 62.9 years) had elevated perioperative liver enzymes (GGT, AST, ALT), and a variety of comorbidities (steatosis 60%, steatohepatitis 33.3%, fibrosis 66.6%) and all received neoadjuvant chemotherapy prior to surgery. A detailed breakdown of patient group characteristics can be found in Supplementary Table 1 and a scheme of the study design and sample processing workflow is given in Figure 1.

 doi:10.20944/preprints202408.2181.v1

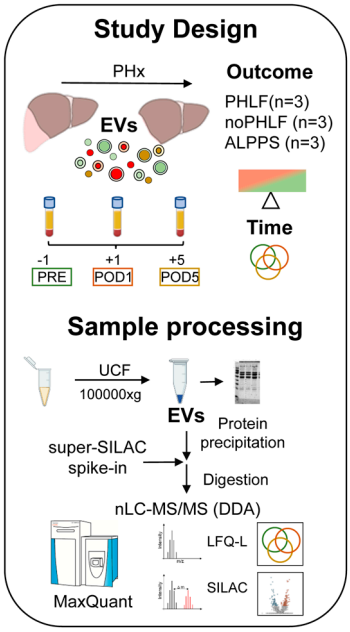

Figure 1. Study design and workflow of sample processing for proteomic analysis of plasma EVs.

2.2. Qualitative Proteome Signatures of Plasma EVs

Initial estimation of proteome quality and complexity was judged by SDS-PAGE profiles and indicated that albumin (70kDa) was prominently present in EVs. Individual protein identifications of each sample are denoted to SDS-PAGE gels and common and unique proteins identified in respective groups (PHLF, noPHLF, ALPPS) are shown in Venn diagrams (Figure 2A). Overall, we identified 2625 (LFQ-L) and 2570 (SILAC) proteins across all the samples with an average of 50% missing values in each sample as illustrated in a heatmap (Suppl. Figure 1A). A detailed analysis of LFQ-L versus SILAC-only proteins in regard to plasma proteins is described in "Data analysis" section (Suppl. Figure 1B-D, Suppl. Data 1 and 2). GOCC-categorization of all identified EV-proteins illustrated in a pie-chart indicated a higher proportion of nuclear proteins (29%) and a small fraction of lysosomal proteins (1%) while other compartments were comparably (10-13%) present in EVs as shown in Figure2B and their percentual share of the total intensity is depicted in Suppl. Figure1D and E. We evaluated the contribution of blood-plasma proteins categorized into complement (25), acute phase proteins (12), coagulation and fibrinolysis (13), lipoproteins (15) as well as typical Vesiclepedia-denoted proteins (81) in regard to the overall EVs protein intensities. This analysis showed that i) the intensity of blood proteins contributed on average to 1% to the total intensity, except for complement (2%), and the intensity for Vesiclepedia-proteins was hightes (8%) and ii) their abundance levels fluctuated most before (PRE) and after (POD5) PHx (Suppl. Figure 2 and Suppl. Data 1).

 doi:10.20944/preprints202408.2181.v1

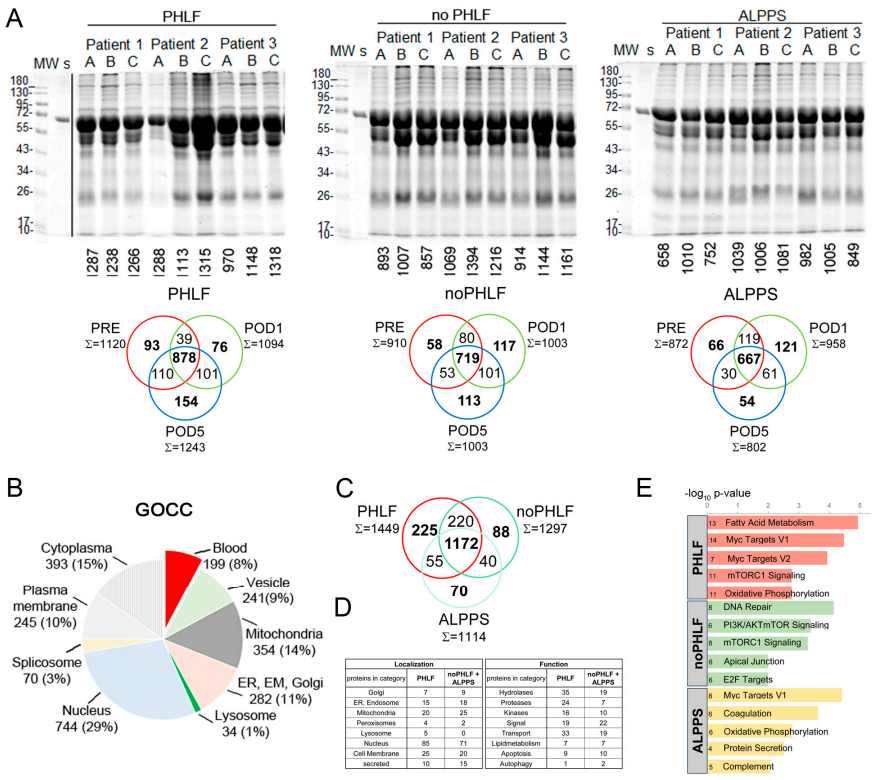

Figure 2. Qualitative proteome signatures of plasma EVs: A) SDS-PAGE protein profiles with number of identified proteins in LC-MS analysis denoted to individual samples (A=before PHx, PRE; B=1 day after PHx, POD1; C= 5 days after PHx, POD5) and Venn diagrams showing common and unique proteins identified in respective sample groups (PHLF, noPHLF, ALPPS) after filtering for at least 2 valid values on the basis of LFQ-L intensities. **B)** GOCC-categorization of all identified proteins. **C)** Venn diagram on overlapping and "only" proteins identified in outcome-groups PHLF, noPHLF and ALPPS irrespective of sampling time after filtering for at least 3 valid values (LFQ-L intensities). Corresponding source data can be found in Suppl. Data 1: **D)** Localization and functional categorization on the basis of Uniprot-Keywords of proteins identified only in PHLF (225), or noPHLF and ALPPS (198). **E)** Top five enriched Molecular Signatures of proteins only identified in PHLF, noPHLF or ALPPS with –log10 p-Values on the x-axis and numbers of proteins in each category denoted. Corresponding source data can be found in Suppl. Data 2.

Since proteins detectable in only one condition are not amenable to comparative statistical analysis, we analysed the overlaps of these unique "only" proteins in each group (considering outcome alone or in combination with time) beforehand. Proteins present in EVs specifically in PHLF, noPHLF or ALPPS irrespective of sampling time (PRE, POD1, POD5) are condensed in Venn diagrams (Figure 2C) with their localization and functions categorized on the basis of Uniprot-Keywords as summarized in Figure 2 D. Nuclear proteins were prominent in both PHLF and noPHLF+ALPPS EVs (85/71), followed by mitochondrial (20/25), cell membrane (25/20), Golgi (7/9), ER and Endosome (15/18) peroxisomal (4/2) and secreted (10/15) proteins. Noticeable, lysosomal proteins (CTSB, GAA, CTSA, VAMP7 and LAMTOR1) were only present in PHLF-EVs. Functional classification revealed that hydrolases, proteases, kinases and proteins with transport functions were prominent in PHLF EVs (35/19, 24/7, 16/10 and 33/19). Proteins with *(paracrine)* signal functions present in PHLF-EVs (19) included leukocyte (ALCAM/CD166), T-cell, endothelial and platelet activation cell surface glycoprotein CD109, the regulator of extracellular glutathione, GGT1 [37] or MCFD2, essential in transport of the coagulation factors FV and FVIII [38] and described to be secreted in EVs in HCC [39] for example. Proteins with assigned with signal function in noPHLF and ALPPS (22) included CD14, CD47, ITGB3/CD61 and ITGA2/CD49B cell surface markers, the hepatocyte growth factor-like protein MST1, TGFB-induced protein TGFBI, selenoprotein P (SEPP1) or the Vitamin K-dependent coagulation regulator PROZ, presumably reflecting the originating cell

 doi:10.20944/preprints202408.2181.v1

type. We found similar numbers of proteins implicated in apoptotic pathways in PHLF/noPHLF and ALPPS (9/10), however, functionally they may act at different levels and fine tune death versus survival decision programs. In PHLF for example, we identified the proapoptotic DDX47 and PAWR (PRKC apoptosis WT1 regulator protein) as well as the antiapoptotic Bax inhibitor 1 (TMBIM6). In noPHLF and ALPPS, apoptosis executioner proteins ACIN1 and TIAL1 (Nucleolysin TIAR), the ferroptosis mediator MTCH1 (Mitochondrial carrier homolog 1) and the antiapoptotic PDCD4, and CISD2 (CDGSH iron-sulfur domain-containing protein 2) proteins were present in EVs. Notably, ER-lipid raft proteins ERLIN1 and ERLIN-2 were only present in noPHLF EVs. An integrative analysis of all "only" proteins revealed unique and overlapping molecular signatures (MSig) in PHLF, noPHLF or ALPPs EVs including Fatty Acid Metabolism, Myc Targets V1/V2, DNA-repair, mTORC1 Signaling or Oxidative phosphorylation for example as depicted in Figure 2E. Details on proteins in respective pathways are summarized in Suppl. Data 2 and enriched protein-protein-interaction network modules are shown in Suppl. Figure 3.

The overlaps of "only" proteins shown in Venn diagrams in Figure 2A were further compared between outcome groups for PRE, POD1 and POD5 separately with analysis results provided in Suppl. Figure 4A. Before PHx (PRE), 86, 67 and 136 EV-proteins were unique to PHLF, noPHLF and ALPPS, respectively. At POD1, 54,150 and 45 EV-proteins were unique to PHLF, noPHLF and ALPPS and at POD5, 60,99 and 93 were unique to PHLF, noPHLF and ALPPS. Proteins with highest LFQ-L abundance (Top5) are listed in a table (Suppl. Figure4B). For example, PRE-PHLF-EV-specific proteins included coagulation factor F12, the proinflammatory cytokine IL18 or STAT1, a key regulator in interferon-signaling. The mannan-binding lectin serine protease 2 (MASP2) and Ficolin-2 (FCN2), coordinately known to activate the lectin complement pathway, were only found at POD1-PHLF-EVs and high mobility group box proteins HMGB1 and 2 were only found in POD5-PHLF-EVs only. Proteins only detected in PRE-noPHLF-EVs included KEAP1, ADAMTS13, BMP1 and the adenylyl cyclase inhibitory Gai subfamily of heteromeric G-proteins (GNA1,2,3). In POD1-noPHLF-EVs, oxidative stress reducing proteins SOD2, gluthathionperoxidase1 (GPX1) or the prenylcysteine oxidase-like PCYOX1 (recently shown to be adipocyte specific EV-cargo, [40] were unique while the tyrosine protein kinases YES, SRC and LYN or the antioxidant selenoprotein Thioredoxin reductase 1 (TXNRD1) were unique to POD5-PHLF-EVs for example. Unique proteins detected in PRE-ALPPS-EVs included the hepatocyte growth factor-like protein MST1, MASP2 or the small GTPases RAP1A/1B as well as secretion associated GTPases SAR1A/1B. Proteins implicated in oxidative stress response including FTH1, Deoxyribose-phosphate aldolase (DERA) or Argininosuccinate synthase (ASS1), were detected POD1-ALPPS-EVs. The hypoxia associated protein Stonin-2, the calcium binding and alarmin protein S100A7 or the procoagulant Kallikrein KLKB1 were detected in POD5-ALPPS-EVs only and shown do be present in EVs earlier [41–44].

2.3. Quantitative Proteome Signatures of Plasma EVs

Principle component analyses (PCA) on EV proteomes in regard to outcome illustrated a higher heterogeneity in noPHLF and ALPPS as compared to PHLF samples (Figure 3A). Following the analysis scheme outlined in Figure 3B, pairwise comparisons of PHLF versus noPHLF or ALPPS were performed. Differentially expressed proteins (DEPs) were visualized in Volcano plots with proteins meeting the significance criteria (conservative p-value<0.05/-$\log_{10}$>1.3, no multiple testing correction) color coded as shown in Figure 3C and D. In these analyses, 53 proteins were upregulated and 32 proteins were downregulated in PHLF versus noPHLF while in comparisons with ALPPS, 110 proteins were higher in PHLF and 78 proteins were lower in ALPPS-EVs.

 doi:10.20944/preprints202408.2181.v1

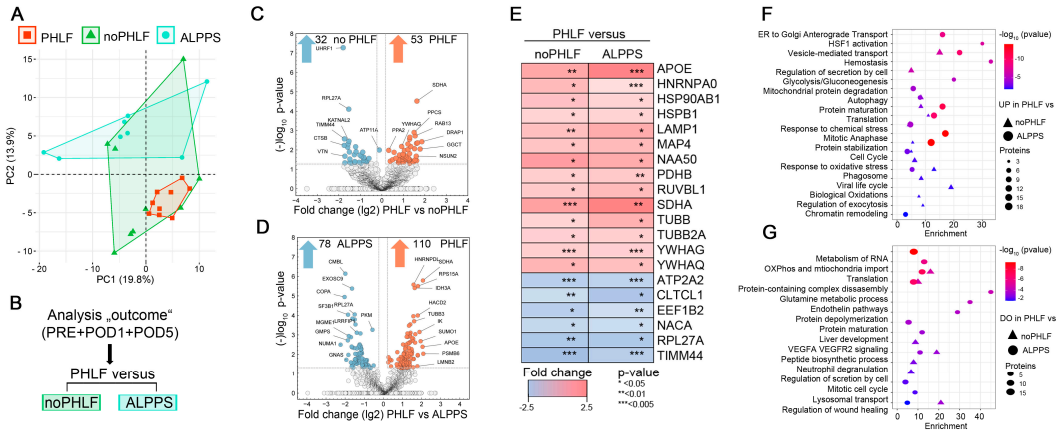

Figure 3. Quantitative proteome signatures of plasma EVs: A) Unsupervised PCA scaled to unit variance of proteins identified in all samples (296) with outcome groups indicated. **B)** Analysis workflow for statistical analysis on differentially expressed proteins (DEPs) on the basis of SILAC ratios. **C, D)** Volcano plots depicting DEPs considering a conservative p-value cutoff ($p<0.05$/-log10 $p>1.3$) as significant. **E)** Heatmap of commonly up- and downregulated proteins in pairwise comparisons of PHLF versus noPHLF or ALPPS. **F, G)** Bubble-plot depicting enriched pathway terms denoted to PHLF-EV proteins significantly up **(F)** or down **(G)** regulated in comparison to both noPHLF and ALPPS. Source data can be found in Suppl Data 3.

Of all significant proteins, we found 14 proteins (APOE, HNRNPA0, HSP90AB1, HSPB1, LAMP1, MAP4, NAA50, PDHB, RUVBL1, SDHA, TUBB, TUBB2A; YWHAG, YWHAQ) commonly up- and 6 proteins (ATP2A2, CLTC1, EEF1B2, NACA4, RPL27A, TIMM44) commonly downregulated in PHLF as illustrated in a heatmap (Figure 3E). Accordingly, PHLF-EVs display increased abundance of metabolic-TCA-cycle-core proteins including pyruvate dehydrogenase beta subunit PDHB, providing acetyl-CoA from glycolysis to TCA and the mitochondrial respiratory chain component succinate-ubiquinone oxidoreductase SDHA, while the abundance of the mitochondrial inner-membrane-to-matrix translocase TIMM44 was reduced, suggesting that EVs reflect mitochondrial dysfunction. We also find increased abundance of phagosome-components (TUBB, TUBB2A and LAMP1) as well as proteins involved in mitotic cell cycle (MAP4, NAA50, RUVBL1) for example. Proteins downregulated in PHLF-EVs included the elongation factor EEF1B2, involved transfer of aminoacylated tRNAs to the ribosome during translation elongation, RPL27A, a protein synthesis component of the 60S ribosome, NACA, a protein binding to nascent polypeptides lacking a signal peptide to prevent mistranslocation to ER as well as reduced abundance of the sarcoplasmic ATPase ATP2A2, involved in transporting cytosolic calcium to ER, altogether indicating disturbed translation, proteostasis and likely unfolded protein response (UPR), which may be further aggravated through abnormal vesicle biogenesis due reduced abundance of the coated pits and vesicle component CTLTC1 for example. A pathway enrichment analysis considering all PHLF-EV 149 upregulated or 104 downregulated proteins after merging comparisons against noPHLF and ALPPS is shown in the bubble-plots in Figure 3F and G. For example, proteins involved in oxidative and chemical stress response (APOE, CAPN2, GSR, LONP1, PRDX2, TXN, ERO1A), hemostasis (C1QBP, MIF, TF, ATP1B1, CAPZA2, AK3 and tubulins) mitochondrial protein degradation (HSPD1, IDH3A, OXCT1, PDHB, SSBP1), or cell cycle (MCM5, PCNA, RAD21, RPA1, MAPRE1) were higher in PHLF-EVs. Proteins assigned to neutrophil degranulation (ANXA2, CTSB, VCP, ATP11A), liver development (ACO2, ASS1, CAD, GMPS) or VEGFA VEGFR2 signaling (DAPZB, LRRFIP2, UBAP2L, KATNAL2) were lower in PHLF-EVs. A complete list of enriched GO terms with proteins involved can be found in Suppl. Data 3.

Of note and in line with our qualitative analysis of EV-cargo (Venn diagrams in Figure 2C and Suppl. Figure4), we found distinct quantitative differences when comparing PHLF versus noPHLF or ALPPS EVs as evident from Volcano plots in Figure 3C and D but also when comparing noPHLF

 doi:10.20944/preprints202408.2181.v1

and ALPPS as further elaborated in GO and PPI network enrichment analysis as shown in Suppl. Figure 5. In these analyses, PHLF-EVs were enriched in signatures assigned to pathways "TP53 regulates metabolic genes" and "Translocation of SLC2A4 (GLUT4) to the plasma membrane" when compared to noPHLF or ALPPS, respectively. In comparisons noPHLF versus ALPPS, "Platelet aggregation" and "Protein kinase A signaling" were higher in ALPPS. Altogether, omitting sampling time (PRE, POD1, POD5) as a parameter in pairwise comparisons provided additional insight into biological processes potentially affected in PHLF patients, including ER stress, compromised protein translation, impaired (intracellular) vesicular transport and mitochondrial dysfunction.

2.4. Predictive EV Signatures for PHLF

In earlier qualitative EV-analysis we found 86 proteins only present in PRE-PHLF – EVs (Suppl. Figure4). Consequently, we finally focused on quantitative differences found in PRE and compared PHLF versus noPHLF or ALPPS, and PCA-plots showed a clear separation, despite of the limited sample size (n=3), Figure 4A. Following comparative statistical analysis, 17 proteins were higher and 12 proteins were lower in PHLF versus noPHLF while 29 proteins were higher and 11 lower in PHLF versus ALPPS (Suppl. Figure6). Only 2 proteins (Heat shock protein beta-1 (HSPB1) and 14-3-3 protein beta/alpha (YWHAB)) were commonly higher in PHLF and one protein (60s ribosomal protein L27a (RPL27A)) lower in PHLF versus noPHLF or ALPPS. In subsequent pathway enrichment analysis, we included "only" proteins (Suppl. Figure4). Accordingly, PHLF-EVs carry signatures assigned to "Metabolism of RNA", "Axon guidance" or "Regulation of proteolysis" while noPHLF or ALPPS-EVs are enriched in proteins assigned to "Hemostasis", "Translation", "Protein maturation", "Wound healing" or "Protein localization to organelle" for example (Figure 4B, C). Taken together these data hint towards a PHLF specific EV signature already prior to surgery.

Figure 4- PHLF-PREdictive EV-signatures

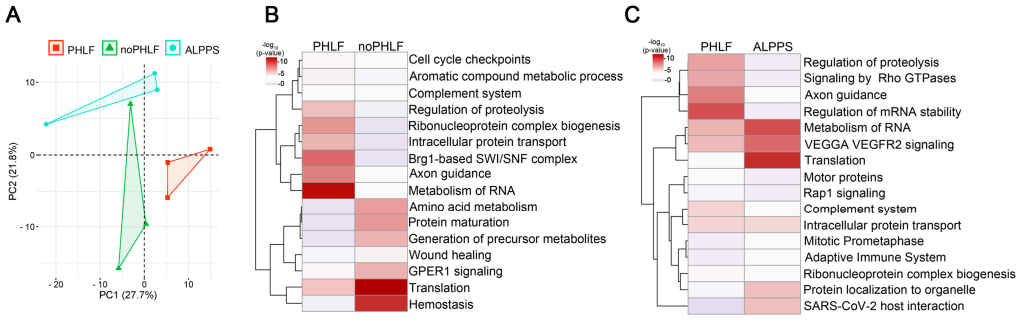

Figure 4. PHLF-PREdictive EV-signatures: A) PCA of EV-protein cargo before (PRE) PHx in outcome groups PHLF, noPHLF and ALPPS. **B, C)** Heatmap summarizing enriched GO-terms of up or downregulated and "only" proteins in PHLF versus noPHLF **(B)** or PHLF versus ALPPS **(C)**. Source data can be found in Suppl. Data 4.

3. Discussion

EVs have emerged as powerful liquid biopsies, capable of reflecting the intricate proteostasis and systemic stress within tissues and organs [7–9] . Their diverse cargo of biomolecules—including proteins, lipids, and nucleic acids—provides a snapshot of the physiological and pathological states of their cells of origin. In fact, EVs are increasingly recognized as treatment option for a variety of diseases, including liver transplantation [46,47]. This makes EVs invaluable for studying complex biological processes, such as liver regeneration and failure, offering insights into the molecular mechanisms at play[45].

In a SILAC-based proteomic analysis of nine HCC patients undergoing PHx, we found that patients who developed PHLF exhibited distinct EV proteome signatures, even before surgery. Our analysis revealed significant dysregulation in pathways related to protein translation, proteostasis, intracellular vesicle biogenesis, metabolic and cell cycle pathways in PHLF-derived EVs. Specifically, proteins involved in mRNA surveillance pathways, the spliceosome, and cell cycle regulation were

 doi:10.20944/preprints202408.2181.v1

notably altered, suggesting underlying issues in translation machinery and vesicular transport processes crucial for cellular homeostasis and tissue regeneration.

The study highlights significant differences in the protein composition of EVs between PHLF patients and those without PHLF treated with ALPPS, indicating distinct cellular and functional characteristics. PHLF-EVs are enriched with lysosomal proteins and those involved in hydrolase, protease, kinase activities, and transport functions, indicating altered cellular processing and signaling in PHLF.

The presence of specific signal proteins in PHLF EVs points to potential paracrine signaling roles contributing to liver pathology and failure. In this regard, we confirmed our recent finding for a role of HMGB1 in PHLF [46], which we find in PHLF-EVs only. Differences in apoptosis-related proteins between groups suggest that regulatory mechanisms of cell death vary between PHLF and noPHLF/ALPPS conditions, as indicated from recent in-vitro works [21].

Additionally, ER-residing lipid raft proteins ERLIN1 and ERLIN2, which respond to sterol depletion and promote autophagosome formation, were found exclusively in noPHLF EVs. This suggests that noPHLF EVs may play a role in counteracting lipid imbalances and enhancing autophagy, contributing to better cellular homeostasis and recovery post-hepatectomy.

Interestingly, EV proteome heterogeneity was higher in noPHLF and ALPPS samples compared to PHLF. Pathway analysis of PHLF proteome signatures highlighted enrichment in cell cycle regulation, vesicle biogenesis, RNA metabolism, and ER stress response, suggesting specific EV proteomic signatures can predict PHLF outcomes, characterized by ER stress and impaired vesicular transport. The proteomic profile of PHLF-derived EVs suggests they might serve as facsimiles of dying hepatocytes and endothelial cells due to the presence of proteins associated with cell death and stress responses in PHLF-derived EVs, contrasting with EVs from regenerative processes that support cell survival, proliferation, and differentiation. Interestingly, these pathological signatures are apparent before PHx, indicating that EVs could serve as predictive tools to determine patients at risk of developing PHLF. The complex interplay of a variety of cell types (re)acting in regenerating liver tissue, including hepatocytes, cholangiocytes, mesenchymal-, endothelial-, and immune cells has recently been resolved at the transcriptional level with single-cell resolution [47]. Each of this cell types naturally secretes proteins packed in EVs in response to stress and/or adaption by unconventional secretion or following cell death. When we overlayed our data with these single-cell transcriptomics data, we find 17 genes (15 hepatocytes and 2 immune cell) with significant higher expression in embolized liver tissue present as proteins exclusively in PHLF-EVs. At the same time, we also find 88 genes assigned to regeneration across all cell types in the “225-only” PHLF-EVs. Furthermore, 19 genes (14 hepatocytes, 5 immune cell) assigned to embolized liver and 68 genes (mostly endothelial cells and cholangiocytes) assigned to regenerating liver were overlapping with 198 proteins only detected in noPHLF and ALPPS-EVs. To which extend the transcriptional landscape corroborates the circulating plasma EV-proteome will be subject of future follow up studies.

Our study is limited in sample size and thus statistical power. We decided to omit imputation of missing values and instead undertook qualitative analysis after careful filtering. By combining longitudinally samples obtained from individuals we were able to diminish intersubject variabilities. From the methodological point of view, our study was limited to ultracentrifugation-based EV purification due to the limited amount of plasma samples, in which co-purification of abundant blood proteins, including lipoproteins or complement for example, is frequently observed [48]. Our study is unique in regard to the SILAC-methodology employed, in which a DDA-dependent acquisition for a subsequent quantification is necessary. As anticipated, typical blood/plasma proteins are not amendable to SILAC labelling. This limitation was alleviated by analyzing the protein´s natural (LFQ-L) signals. Nonetheless, the number of identified plasma EV-proteins identified in this study exceeds all DDA-based proteomic studies considering the limited sample volume used in this study, reaching identification numbers currently achievable only with DIA-methodologies.

Taken together, SILAC-based proteomic characterization of plasma EVs in patients undergoing PHx provides novel insights into the proteomic changes associated with PHLF. The signature of EVs

 doi:10.20944/preprints202408.2181.v1

in patients with PHLF indicates significant disruptions in protein translation and vesicle biogenesis, and mirrors that of dying hepatocytes and endothelial cells, which contrasts with the traditional role of EVs in promoting regeneration in other contexts. These signatures, apparent before surgery, highlight the potential of EVs as predictive biomarkers and suggest avenues for future therapeutic interventions to mitigate liver failure risks.

4. Materials and Methods

Patient Cohort

Patients with HCC were recruited at the Clinic Landstrasse, Vienna between January 2016 and March 2019 [18]. Blood was taken pre-surgery (POP), one (POD1) and five (POD5) days after surgery. Demographics, and laboratory parameters and PHLF (using ISGLS) were assessed [19] Informed consent was obtained, adhering to ethical guidelines, and registered on ClinicalTrials.gov (NCT01921985, NCT01700231; accessed on 5th of July 2024). Morbidity was defined using the criteria put forth by Dindo et al. [20]. Severe morbidity was defined as grade 3 or higher. PHLF was graded based on criteria established by the International Study Group of Liver Surgery. The diagnosis of PHLF was characterized by elevated serum bilirubin (SB) levels and prolonged prothrombin time (PT) persisting on the fifth day after surgery. For patients with abnormal SB and PT levels before surgery, SB had to increase and PT decrease compared to preoperative values to indicate PHLF. Patients who did not undergo routine postoperative blood draws due to good clinical condition or early discharge were classified as not having PHLF.

This study included 3 patients with PHLF, 3 patients undergoing the Associating Liver Partition and Portal vein Ligation for Staged hepatectomy (ALPPS) procedure [21] and three matched controls without complications (noPHLF). CTAD-anticoagulated plasma was collected from the portal vein 1 day perioperatively (PRE) as well as 1 and 5 days after resection of malignant tissue (POD1 and POD5), sequentially centrifuged at 1,000× g and 10,000× g at 4 °C for 10 min to ensure removal of all cellular components [22] and stored in 15ul aliquots at −80 °C until further use. and carefully deposited in a biobank at -80°C.

Isolation of Plasma EVs by Ultracentrifugation

For EV isolation, 110µl plasma were diluted with 1ml PBS and centrifuged at 100.000xg/41.000rpm using a fixed angle TLA45 rotor and an Optima TLX Ultracentrifuge, (Beckman Coulter) for 45min at 16°C. Supernatants were removed by pipetting, EV-pellets were washed by resuspending in 1ml PBS and centrifuged again. EV-pellets were resuspended in a final volume of 50µl PBS, 10µl were used for SDS-PAGE-based (SDS-PAGE) based protein content, quality and complexity estimation while 30µl were subjected to methanol-assisted protein precipitation and delipipdation. For this, 10 volumes (500µl) cold methanol was added, samples were vortex and sonicated for 1min, incubated overnight at -20°C and centrifuged for 20min at 13.000xg and 4°C. The protein pellet was washed by addition of 500µl methanol. After centrifugation, pellets were air-dried and processed for proteomic analysis. Reproducibility of ultracentrifugation-based EV isolation had been proven beforehand with 3 healthy subjects and is available upon request.

Super-SILAC and Sample Preparation for Mass Spectrometry

A heavy isotope-labelled super-SILAC-proteome standard was prepared from a variety of cell types and culturing in SILAC heavy DMEM as described previously [23]. In detail, the HCC cell lines HepG2, Hep3B and Huh7, colorectal cancer cell line HCT116, prostate cancer cell line LnCAP, leukemia and monocytic cell lines HL-60 and U937, the EAhy 926 hybridoma (HUVEC/A549) cell line displaying stable endothelial characteristics as well as primary HUVEC and HAEC were cultured in lysine- and arginine-depleted DMEM supplemented with 10% dialyzed fetal bovine serum and 73 mg/L heavy [$^{13}C_6{}^{15}N_2$) L-lysine and 28 mg/L [$^{13}C_6{}^{15}N_4$] L-arginine (all Silantes) as well as 100U/ml penicillin/streptomycin (Invitrogen). Cells were grown for at least five generations to allow full incorporation of labelled amino acids. Individual cell lysates were prepared in a lysis buffer (4% SDS

 doi:10.20944/preprints202408.2181.v1

in PBS) and SILAC labelling was checked after FASP-digestion [24] and MS analysis as described below. The super-SILAC mix was prepared from a mixture of all cells-lysates and 100ug Methanol-precipitated aliquots were stored at -80°C until use. EV-protein pellets were solubilized in 6M urea and 2M thiourea in HEPES pH 8.0 and mixed with 10µg super-SILAC mixed dissolved in the same buffer. After reduction (10mM DTT) and cystein alkylation (55mM CAA), proteins were sequentially digested with LysC (0.5µl 0.05mg/ml, 3h RT), diluted with 50mM Ammoniumbicarbonate to 2M Urea and incubated with Trypsin (1µl 0.05mg/ml) overnight. Finally, digests were acidified to 1% Formic Acid (FA), desalted and concentrated using C18 stage-Tips [25].

LC-MS/MS Analysis and Raw Data Processing

Peptides were analyzed on a nano UHPLC 1000 (Proxeon) coupled via a nanoelectrospray ionization source to a Q-Exactive™ Orbitrap™ mass spectrometer (Thermo Fisher Scientific) operating in a top 12 data-dependent mode (DDA) as described but using a 2h gradient [26]. Raw files were initially processed with MaxQuant (v 1.5.3.8, 2016) and (v2.1.3.0 2024) with MS/MS spectra assigned to the human Uniprot database (UP000005640_9606, 20.590 entries) [27]. Default settings for mass tolerance and peptide length were used, enzyme specificity was set to LysC/P and Trypsin/P. Identification and SILAC quantitation settings were set to a min. ratio count of 1, match between, dependent peptides as well as iBAQ and LFQ quantitation was enabled to quantify peptides with a missing MS1/2 and to account for human plasma proteins absent in our super-SILAC mix and to evaluate the original abundance of plasma-EV proteins. N-term acetylation, oxidation (M) and phosphorylation (STY) were set as variable, cystein carbamido-methylation and N-terminal protein acetylation as fixed modification.

Data Analysis

The MaxQuant output (proteingroups.txt) was analyzed using Perseus (v.1.6.15.0) software [28]. SILAC (normalized H/L ratios) and LFQ-L were uploaded and filtered for reverse, potential contaminants, keratins and immunoglobulins (66/90), LFQ-L and SILAC ratios (L/H) were log2 transformed, data distribution was inspected in histograms and data completeness was visualized in heatmaps (Suppl. Figure1A). Sample-groups were annotated (outcome, time and the combination thereof) and proteins were annotated with “lipoproteins”, “complement”, “coagulation”, “acute phase”, “fibrinolysis”, “serpins”, Vesiclepedia Top100 and with Gene Ontology terms for cellular component (GOCC) and Mitocarta 3.0. In anticipation that plasma-specific proteins might be absent in the super-SILAC proteome standard (no SILAC ratio) and appear as missing value (NaN), we compared LFQ-L (2626) and SILAC (2570) protein identifications in Venn diagrams and found that 117 LFQ-L “only” proteins constituted proteins involved in complement activation, immune effector functions and ECM regulation displaying liver hepatocyte, Kupffer cells and lung dendritic signatures while 62 SILAC-only proteins were enriched functions in cell cycle regulation, late endosome to vacuole transport and antiviral response and displayed neuronal cortical stem cell, skeletal muscle and bone marrow pro B cell signatures as illustrated in Venn diagrams and enrichment plots Suppl. Figure 1B and C, Suppl. Data 1. GOCC categorization of proteins in “outcome” and “time” groups are summarized in Suppl. Figure 1D and E. To evaluate the robustness of our SILAC proteome standard, the variance of 3506 proteins with LFQ-H identified across all the samples was found to be 2.4±1.5 % while only 153 proteins had variations higher than 5% (range 5-40.6%) and 11 proteins had a variation higher than 10% (CP, EP400, IGM, IGHM, C5, VWF, NRAS, BPIFC, TMSB10, FGA, FGB, Suppl. Data 1). These 153 proteins were enriched in biological functions such as Eukaryotic Translation Elongation (23 proteins, log(p): -32), Platelet degranulation (13 proteins, log(p): -12.9), ER-Phagosome pathway (10 proteins, log(p): -10.5), mRNA processing (11 proteins, log(p): -7.2), and VEGFA VEGFR2 signaling (15 proteins, log(p): -9.8). Qualitative comparisons of protein identifications in outcome groups were filtered for at least 3 (outcome) or 2 (outcome and time) valid values. SILAC-ratios were centered through median-z-score normalization and pairwise statistical comparisons were performed using two-sided Student T-tests using conservative ($p<0.05$) as well as permutation-based estimation of false discovery rates (250

 doi:10.20944/preprints202408.2181.v1

permutations, FDR cut-off q<0.05). Protein set enrichment analysis were done with open-source tools Metascape [29], Enrichr-KG [30]and GSEA [31–33]. Graphical visualizations were done in Instant Clue [34], SRplot [35], Cytoscape v3.10.1 [36], GraphPad-Prism (v.8.0) and Excel.

Supplementary Materials: The following supporting information can be downloaded at the website of this paper posted on Preprints.org., Figure S1: Qualitative comparison of LFQ-L and SILAC identifications to capture plasma specific proteins ; Figure S2 : Blood- and Vesiclepedia proteins identified and quantified in plasma EVs; Figure S3: Enriched protein-protein-interaction (PPI) network modules in EVs; Figure S4: Unique proteins in sampling time and outcome groups; Figure S5: EV-protein cargo signatures discriminating PHLF from noPHLF and ALPPS; Figure S6: PREdictive outcome signatures; Supplementary Data files: Suppl Data 01.xlsx; Suppl Data 02.xlsx, Suppl Data 03.xlsx, Suppl Data 04.xlsx.

Author Contributions: Conception and experimental design: U.R., M.K., P.S. and A.A.; Experimental work and analyzes: U.R., D.P., J.S.; H.H. and L.B.; Manuscript writing: U.R. and A.A.; Sample collection and data analysis: D.P., J.S., J.P., A.S.J., M.A. and H.H.; Manuscript editing: H.H., D.P., J.S., L.B., J.P., V.L., A.S.F., M.A., M.K. and P.S. All authors have read and agreed to the published version of the manuscript.

Funding: The study was funded by the NIH (R01DK122813) and the Austrian Science Fund (FWF) P-32064 and P-34783. For the purpose of open access, the author has applied a CC BY public copyright licence to any Author Accepted Manuscript version arising from this submission.

Institutional Review Board Statement: The study was conducted in accordance with the Declaration of Helsinki and registered on ClinicalTrials.gov (NCT01921985, NCT01700231; accessed on 5th of July 2024).

Data Availability Statement: All data needed to evaluate the conclusions in the paper are present in the paper and/or the Supplementary Materials.

Acknowledgments: We thank the CECAD/CMMC-Proteomics Facility team members Astrid-Wilbrand Hennes, Jan Krueger, Ursula Cullmann, Christian Frese and Stefan Müller for analytical assistance, Marcus Krueger lab-members Sebastian Kallabis, Clara Türk and Janica Lea Wiederstein for sharing their workbenches and Matthias Mann for advice in regard to super-SILAC mix and Manolis Pasparakis (CECAD, Institute for Genetics, University of Cologne) generously providing SILAC-media.

Conflicts of Interest: The authors declare no conflicts of interest.

References

1. Sparrelid, E.; Olthof, P.B.; Dasari, B.V.M.; Erdmann, J.I.; Santol, J.; Starlinger, P.; Gilg, S. Current Evidence on Posthepatectomy Liver Failure: Comprehensive Review. *BJS Open* **2022**, *6*, zrac142, doi:10.1093/bjsopen/zrac142.
2. Haegele, S.; Reiter, S.; Wanek, D.; Offensperger, F.; Pereyra, D.; Stremitzer, S.; Fleischmann, E.; Brostjan, C.; Gruenberger, T.; Starlinger, P. Perioperative Non-Invasive Indocyanine Green-Clearance Testing to Predict Postoperative Outcome after Liver Resection. *PLoS One* **2016**, *11*, e0165481, doi: 10.1371/journal.pone.0165481.
3. Santol, J.; Ammann, M.; Reese, T.; Kern, A.E.; Laferl, V.; Oldhafer, F.; Dong, Y.; Rumpf, B.; Vali, M.; Wiemann, B.; et al. Comparison of the LiMAx Test vs. the APRI+ALBI Score for Clinical Utility in Preoperative Risk Assessment in Patients Undergoing Liver Surgery – A European Multicenter Study. *European Journal of Surgical Oncology* **2024**, *50*, 108048, doi: 10.1016/j.ejso.2024.108048.
4. Santol, J.; Kim, S.; Gregory, L.A.; Baumgartner, R.; Murtha-Lemekhova, A.; Birgin, E.; Gloor, S.; Braunwarth, E.; Ammann, M.; Starlinger, J.; et al. An APRI+ALBI Based Multivariable Model as Preoperative Predictor for Posthepatectomy Liver Failure. *Ann Surg* **2023**, doi:10.1097/SLA.0000000000006127.
5. Schwarz, C.; Plass, I.; Fitschek, F.; Punzengruber, A.; Mittlböck, M.; Kampf, S.; Asenbaum, U.; Starlinger, P.; Stremitzer, S.; Bodingbauer, M.; et al. The Value of Indocyanine Green Clearance Assessment to Predict Postoperative Liver Dysfunction in Patients Undergoing Liver Resection. *Sci Rep* **2019**, *9*, 8421, doi:10.1038/s41598-019-44815-x.
6. Abu Rmilah, A.; Zhou, W.; Nelson, E.; Lin, L.; Amiot, B.; Nyberg, S.L. Understanding the Marvels behind Liver Regeneration. *Wiley Interdiscip Rev Dev Biol* **2019**, *8*, e340, doi:10.1002/wdev.340.
7. van Niel, G.; D'Angelo, G.; Raposo, G. Shedding Light on the Cell Biology of Extracellular Vesicles. *Nat Rev Mol Cell Biol* **2018**, *19*, 213–228, doi:10.1038/nrm.2017.125.
8. Raposo, G.; Stoorvogel, W. Extracellular Vesicles: Exosomes, Microvesicles, and Friends. *J Cell Biol* **2013**, *200*, 373–383, doi:10.1083/jcb.201211138.

9. Berumen Sánchez, G.; Bunn, K.E.; Pua, H.H.; Rafat, M. Extracellular Vesicles: Mediators of Intercellular Communication in Tissue Injury and Disease. *Cell Communication and Signaling* **2021**, *19*, 104, doi:10.1186/s12964-021-00787-y.
10. Castaño, C.; Novials, A.; Párrizas, M. An Overview of Inter-Tissue and Inter-Kingdom Communication Mediated by Extracellular Vesicles in the Regulation of Mammalian Metabolism. *IJMS* **2023**, *24*, 2071, doi:10.3390/ijms24032071.
11. Dickhout, A.; Koenen, R.R. Extracellular Vesicles as Biomarkers in Cardiovascular Disease; Chances and Risks. *Frontiers in Cardiovascular Medicine* **2018**, *5*, doi:10.3389/fcvm.2018.00113.
12. Hill, A.F. Extracellular Vesicles and Neurodegenerative Diseases. *J. Neurosci.* **2019**, *39*, 9269–9273, doi:10.1523/JNEUROSCI.0147-18.2019.
13. Michel, L.Y.M. Extracellular Vesicles in Adipose Tissue Communication with the Healthy and Pathological Heart. *IJMS* **2023**, *24*, 7745, doi:10.3390/ijms24097745.
14. Yang, Q.; Xu, J.; Gu, J.; Shi, H.; Zhang, J.; Zhang, J.; Chen, Z.-S.; Fang, X.; Zhu, T.; Zhang, X. Extracellular Vesicles in Cancer Drug Resistance: Roles, Mechanisms, and Implications. *Advanced Science* **2022**, *9*, 2201609, doi:10.1002/advs.202201609.
15. Yoshida, M.; Satoh, A.; Lin, J.B.; Mills, K.F.; Sasaki, Y.; Rensing, N.; Wong, M.; Apte, R.S.; Imai, S.-I. Extracellular Vesicle-Contained eNAMPT Delays Aging and Extends Lifespan in Mice. *Cell Metab* **2019**, *30*, 329-342.e5, doi:10.1016/j.cmet.2019.05.015.
16. Cheng, L.; Hill, A.F. Therapeutically Harnessing Extracellular Vesicles. *Nat Rev Drug Discov* **2022**, *21*, 379–399, doi:10.1038/s41573-022-00410-w.
17. Lu, W.; Tang, H.; Li, S.; Bai, L.; Chen, Y. Extracellular Vesicles as Potential Biomarkers and Treatment Options for Liver Failure: A Systematic Review up to March 2022. *Frontiers in Immunology* **2023**, *14*.
18. Starlinger, P.; Brunnthaler, L.; McCabe, C.; Pereyra, D.; Santol, J.; Steadman, J.; Hackl, M.; Skalicky, S.; Hackl, H.; Gronauer, R.; et al. Transcriptomic Landscapes of Effective and Failed Liver Regeneration in Humans. *JHEP Reports* **2023**, *5*, 100683, doi: 10.1016/j.jhepr.2023.100683.
19. Rahbari, N.N.; Garden, O.J.; Padbury, R.; Brooke-Smith, M.; Crawford, M.; Adam, R.; Koch, M.; Makuuchi, M.; Dematteo, R.P.; Christophi, C.; et al. Posthepatectomy Liver Failure: A Definition and Grading by the International Study Group of Liver Surgery (ISGLS). *Surgery* **2011**, *149*, 713–724, doi: 10.1016/j.surg.2010.10.001.
20. Dindo, D.; Demartines, N.; Clavien, P.-A. Classification of Surgical Complications: A New Proposal with Evaluation in a Cohort of 6336 Patients and Results of a Survey. *Ann Surg* **2004**, *240*, 205–213, doi: 10.1097/01.sla.0000133083.54934.ae.
21. Brandel, V.; Schimek, V.; Göber, S.; Hammond, T.; Brunnthaler, L.; Schrottmaier, W.C.; Mussbacher, M.; Sachet, M.; Liang, Y.Y.; Reipert, S.; et al. Hepatectomy-Induced Apoptotic Extracellular Vesicles Stimulate Neutrophils to Secrete Regenerative Growth Factors. *Journal of Hepatology* **2022**, *77*, 1619–1630, doi: 10.1016/j.jhep.2022.07.027.
22. Mussbacher, M.; Krammer, T.L.; Heber, S.; Schrottmaier, W.C.; Zeibig, S.; Holthoff, H.-P.; Pereyra, D.; Starlinger, P.; Hackl, M.; Assinger, A. Impact of Anticoagulation and Sample Processing on the Quantification of Human Blood-Derived microRNA Signatures. *Cells* **2020**, *9*, 1915, doi:10.3390/cells9081915.
23. Geiger, T.; Wisniewski, J.R.; Cox, J.; Zanivan, S.; Kruger, M.; Ishihama, Y.; Mann, M. Use of Stable Isotope Labeling by Amino Acids in Cell Culture as a Spike-in Standard in Quantitative Proteomics. *Nat Protoc* **2011**, *6*, 147–157, doi:10.1038/nprot.2010.192.
24. Wiśniewski, J.R.; Zougman, A.; Nagaraj, N.; Mann, M. Universal Sample Preparation Method for Proteome Analysis. *Nat Methods* **2009**, *6*, 359–362, doi:10.1038/nmeth.1322.
25. Rappsilber, J.; Mann, M.; Ishihama, Y. Protocol for Micro-Purification, Enrichment, Pre-Fractionation and Storage of Peptides for Proteomics Using StageTips. *Nat Protoc* **2007**, *2*, 1896–1906, doi:10.1038/nprot.2007.261.
26. Nolte, H.; Hölper, S.; Selbach, M.; Braun, T.; Krüger, M. Assessment of Serum Protein Dynamics by Native SILAC Flooding (SILflood). *Anal. Chem.* **2014**, *86*, 11033–11037, doi:10.1021/ac502883p.
27. Cox, J.; Mann, M. MaxQuant Enables High Peptide Identification Rates, Individualized p.p.b.-Range Mass Accuracies and Proteome-Wide Protein Quantification. *Nat Biotechnol* **2008**, *26*, 1367–1372, doi:10.1038/nbt.1511.
28. Tyanova, S.; Temu, T.; Sinitcyn, P.; Carlson, A.; Hein, M.Y.; Geiger, T.; Mann, M.; Cox, J. The Perseus Computational Platform for Comprehensive Analysis of (Prote)Omics Data. *Nat Methods* **2016**, *13*, 731–740, doi:10.1038/nmeth.3901.
29. Zhou, Y.; Zhou, B.; Pache, L.; Chang, M.; Khodabakhshi, A.H.; Tanaseichuk, O.; Benner, C.; Chanda, S.K. Metascape Provides a Biologist-Oriented Resource for the Analysis of Systems-Level Datasets. *Nat Commun* **2019**, *10*, 1523, doi:10.1038/s41467-019-09234-6.

30. Kuleshov, M.V.; Jones, M.R.; Rouillard, A.D.; Fernandez, N.F.; Duan, Q.; Wang, Z.; Koplev, S.; Jenkins, S.L.; Jagodnik, K.M.; Lachmann, A.; et al. Enrichr: A Comprehensive Gene Set Enrichment Analysis Web Server 2016 Update. *Nucleic Acids Res* **2016**, *44*, W90-97, doi:10.1093/nar/gkw377.
31. Sherman, B.T.; Hao, M.; Qiu, J.; Jiao, X.; Baseler, M.W.; Lane, H.C.; Imamichi, T.; Chang, W. DAVID: A Web Server for Functional Enrichment Analysis and Functional Annotation of Gene Lists (2021 Update). *Nucleic Acids Res* **2022**, *50*, W216–W221, doi:10.1093/nar/gkac194.
32. Xie, Z.; Bailey, A.; Kuleshov, M.V.; Clarke, D.J.B.; Evangelista, J.E.; Jenkins, S.L.; Lachmann, A.; Wojciechowicz, M.L.; Kropiwnicki, E.; Jagodnik, K.M.; et al. Gene Set Knowledge Discovery with Enrichr. *Current Protocols* **2021**, *1*, e90, doi:10.1002/cpz1.90.
33. Subramanian, A.; Tamayo, P.; Mootha, V.K.; Mukherjee, S.; Ebert, B.L.; Gillette, M.A.; Paulovich, A.; Pomeroy, S.L.; Golub, T.R.; Lander, E.S.; et al. Gene Set Enrichment Analysis: A Knowledge-Based Approach for Interpreting Genome-Wide Expression Profiles. *Proceedings of the National Academy of Sciences* **2005**, *102*, 15545–15550, doi:10.1073/pnas.0506580102.
34. Nolte, H.; MacVicar, T.D.; Tellkamp, F.; Krüger, M. Instant Clue: A Software Suite for Interactive Data Visualization and Analysis. *Sci Rep* **2018**, *8*, 12648, doi:10.1038/s41598-018-31154-6.
35. Tang, D.; Chen, M.; Huang, X.; Zhang, G.; Zeng, L.; Zhang, G.; Wu, S.; Wang, Y. SRplot: A Free Online Platform for Data Visualization and Graphing. *PLOS ONE* **2023**, *18*, e0294236, doi: 10.1371/journal.pone.0294236.
36. Shannon, P.; Markiel, A.; Ozier, O.; Baliga, N.S.; Wang, J.T.; Ramage, D.; Amin, N.; Schwikowski, B.; Ideker, T. Cytoscape: A Software Environment for Integrated Models of Biomolecular Interaction Networks. *Genome Res* **2003**, *13*, 2498–2504, doi:10.1101/gr.1239303.
37. Kawakami, K.; Fujita, Y.; Matsuda, Y.; Arai, T.; Horie, K.; Kameyama, K.; Kato, T.; Masunaga, K.; Kasuya, Y.; Tanaka, M.; et al. Gamma-Glutamyltransferase Activity in Exosomes as a Potential Marker for Prostate Cancer. *BMC Cancer* **2017**, *17*, 316, doi:10.1186/s12885-017-3301-x.
38. Nyfeler, B.; Zhang, B.; Ginsburg, D.; Kaufman, R.J.; Hauri, H.-P. Cargo Selectivity of the ERGIC-53/MCFD2 Transport Receptor Complex. *Traffic* **2006**, *7*, 1473–1481, doi:10.1111/j.1600-0854.2006.00483. x.
39. He, M.; Qin, H.; Poon, T.C.W.; Sze, S.-C.; Ding, X.; Co, N.N.; Ngai, S.-M.; Chan, T.-F.; Wong, N. Hepatocellular Carcinoma-Derived Exosomes Promote Motility of Immortalized Hepatocyte through Transfer of Oncogenic Proteins and RNAs. *Carcinogenesis* **2015**, *36*, 1008–1018, doi:10.1093/carcin/bgv081.
40. Garcia-Martin, R.; Brandao, B.B.; Thomou, T.; Altindis, E.; Kahn, C.R. Tissue Differences in the Exosomal/Small Extracellular Vesicle Proteome and Their Potential as Indicators of Altered Tissue Metabolism. *Cell Rep* **2022**, *38*, 110277, doi: 10.1016/j.celrep.2021.110277.
41. Herrera Sanchez, M.B.; Previdi, S.; Bruno, S.; Fonsato, V.; Deregibus, M.C.; Kholia, S.; Petrillo, S.; Tolosano, E.; Critelli, R.; Spada, M.; et al. Extracellular Vesicles from Human Liver Stem Cells Restore Argininosuccinate Synthase Deficiency. *Stem Cell Res Ther* **2017**, *8*, 176, doi:10.1186/s13287-017-0628-9.
42. Głuszko, A.; Szczepański, M.J.; Whiteside, T.L.; Reichert, T.E.; Siewiera, J.; Ludwig, N. Small Extracellular Vesicles from Head and Neck Squamous Cell Carcinoma Cells Carry a Proteomic Signature for Tumor Hypoxia. *Cancers (Basel)* **2021**, *13*, 4176, doi:10.3390/cancers13164176.
43. Kalra, H.; Adda, C.G.; Liem, M.; Ang, C.-S.; Mechler, A.; Simpson, R.J.; Hulett, M.D.; Mathivanan, S. Comparative Proteomics Evaluation of Plasma Exosome Isolation Techniques and Assessment of the Stability of Exosomes in Normal Human Blood Plasma. *Proteomics* **2013**, *13*, 3354–3364, doi:10.1002/pmic.201300282.
44. Whitham, M.; Parker, B.L.; Friedrichsen, M.; Hingst, J.R.; Hjorth, M.; Hughes, W.E.; Egan, C.L.; Cron, L.; Watt, K.I.; Kuchel, R.P.; et al. Extracellular Vesicles Provide a Means for Tissue Crosstalk during Exercise. *Cell Metab* **2018**, *27*, 237-251.e4, doi: 10.1016/j.cmet.2017.12.001.
45. Lu, W.; Tang, H.; Li, S.; Bai, L.; Chen, Y. Extracellular Vesicles as Potential Biomarkers and Treatment Options for Liver Failure: A Systematic Review up to March 2022. *Front Immunol* **2023**, *14*, 1116518, doi:10.3389/fimmu.2023.1116518.
46. Brunnthaler, L.; Hammond, T.G.; Pereyra, D.; Santol, J.; Probst, J.; Laferl, V.; Resch, U.; Aiad, M.; Janoschek, A.S.; Gruenberger, T.; et al. HMGB1-Mediated Cell Death-A Crucial Element in Post-Hepatectomy Liver Failure. *Int J Mol Sci* **2024**, *25*, 7150, doi:10.3390/ijms25137150.
47. Brazovskaja, A.; Gomes, T.; Holtackers, R.; Wahle, P.; Körner, C.; He, Z.; Schaffer, T.; Eckel, J.C.; Hänsel, R.; Santel, M.; et al. Cell Atlas of the Regenerating Human Liver after Portal Vein Embolization. *Nat Commun* **2024**, *15*, 5827, doi:10.1038/s41467-024-49236-7.
48. Holcar, M.; Kandušer, M.; Lenassi, M. Blood Nanoparticles – Influence on Extracellular Vesicle Isolation and Characterization. *Front Pharmacol* **2021**, *12*, 773844, doi:10.3389/fphar.2021.773844.

 doi:10.20944/preprints202408.2181.v1

disclaim responsibility for any injury to people or property resulting from any ideas, methods, instructions or products referred to in the content.